

Individual Treatment Effect Estimation in a Low Compliance Setting

Thibaud Rahier, Amélie Héliou, Matthieu Martin,
Christophe Renaudin and Eustache Diemert

Criteo AI Lab

Abstract

Individual Treatment Effect (ITE) estimation is an extensively researched problem, with applications in various domains. We model the case where there is heterogeneous non-compliance to a randomly assigned treatment, a typical situation in health (because of non-compliance to prescription) or digital advertising (because of competition and ad blockers for instance). The lower the compliance, the more the effect of treatment prescription – or individual prescription effect (IPE) – signal fades away and becomes hard to capture. We propose a new approach to estimate IPE that takes advantage of observed compliance information to prevent signal fading. Using the Structural Causal Model framework and do-calculus, we define a general mediated causal effect setting under which our proposed estimator soundly recovers the IPE, and study its asymptotic variance. Finally, we conduct extensive experiments on both synthetic and real-world datasets that highlight the benefit of the approach, which consistently improves state-of-the-art in low compliance settings.

1 Introduction

Individual Treatment Effect (ITE) estimation is an important task in various applications such as healthcare Foster et al. (2011), online advertising Diemert et al. (2018) and socio-economics Xie et al. (2012). As it is often the case in practice, we assume that we cannot directly control the treatment intake but only the treatment prescription (or assignment): we therefore focus on the Individual Prescription Effect (IPE), which designates the effect of the treatment prescription T on the outcome Y , conditionally to context X (*c.f.* Equation (1), assuming randomized treatment prescription).

$$IPE(x) = \mathbb{E}[Y|X = x, T = 1] - \mathbb{E}[Y|X = x, T = 0] \quad (1)$$

We also assume that we observe the treatment intake (or equivalently, the compliance to prescription), which we denote M since it acts as a mediator of the causal effect of T on Y . The effect of M on Y will henceforth be referred to as ITE.

Table 1 illustrates various settings in which non-compliance to treatment prescription may occur (Gordon et al., 2019; Jin et al., 2008; Parker, 2000). This happens for instance when individuals have the choice not to abide by the prescription or if there exists conflicting interests. Of course one can choose to focus the study on actually treated individuals only (ITE). But from a decision making point of view it often makes sense to consider that future treatment decisions need to take into account the possibility of non-compliance so as to accurately predict future expected outcomes. For example a policy maker would want to take into account that not all individuals would abide by the new policy (as can be estimated from a pilot study) to predict the expected impact of a roll-out of said policy.

Now we argue that IPE estimation can be hampered by non-compliance. Firstly note that individuals who did not receive the treatment contribute only noise to the default IPE estimator as their observed

Table 1: Examples of covariates (X), outcome (Y), treatment prescription (T), reason for not abiding to treatment (R) and evidence of treatment acceptance (M)

VAR.	MEDICINE	ONLINE ADV.	JOB TRAINING
X	PATIENT INFO	PURCHASE HISTORY	SCHOOLING
T	DRUG PRESCRIPTION	BID PLACEMENT	TRAINING OFFER
R	RELUCTANCE	COMPETITION	DISEASE
M	DRUG INTAKE	AD DISPLAYED	TRAINING DONE
Y	RECOVERY	SALE/VISIT	EMPLOYMENT

outcome is not effectively influenced. Therefore the variance of the estimator increases when the compliance level decreases. A classical move in statistics would be to build a stratified estimator on the treatment variable. But we will see in Section 3 that even when observing data from a randomized experiment one needs additional assumptions to build a consistent estimator that recovers the causal effect of T on Y .

Besides, in the literature ITE models (also called *uplift* models in marketing literature) are often considered as prescriptive tools. Indeed, treatment effect predictions are used in order to target treatment to individuals for which it is the most beneficial (Devriendt et al., 2018; Radcliffe & Surry, 2011). This calls for an evaluation metric that measures by how much the average treatment effect would have been improved had the treatment been targeted not by a random instrument, but by ITE predictions instead. For that purpose (Rzepakowski & Jaroszewicz, 2012, 2010; Radcliffe & Surry, 2011) have proposed the Area Under the Uplift Curve (AUUC) metric that sums the benefits over individuals ranked by predictions. An interesting property of this metric is that it can be used on real data for which we observe a given individual in either treated or untreated conditions but never both.

Confronted with the challenges of i) learning IPE models in conditions of (possibly high) non-compliance and ii) evaluating them as prescriptive tools we propose to pose the problem in the setting of causal inference and derive an IPE estimator that takes advantage of observed compliance. Our main contributions are as follows.

1. Formalization of IPE estimation in a setting of observed compliance described using structural causal models, which extends to more general cases of mediated causal effect estimation (Section 3)
2. Proposition of a meta-estimator (in which can be plugged any ITE estimator) improving robustness of classical causal effect estimators to (high) non-compliance settings, proof of consistency (Section 4.1) and asymptotic variance properties (Section 4.2)
3. Thorough empirical evaluation of this meta-estimator on synthetic and real world datasets (Section 5)

2 Related works

We review three main domains that are concerned with research questions similar to our work: ITE modeling, non compliance in causal inference and evaluation metrics for ITE modeling.

First, we note that ITE models are a pervasive concept in different research fields such as marketing - under the name uplift models Radcliffe & Surry (2011), statistics - as conditional average treatment effect estimators Künzel et al. (2019) or econometrics - heterogeneous treatment effect models (Jacob et al., 2019; Wager & Athey, 2018). A simple yet highly scalable approach consists in learning a regression of Y on X separately in both treatment ($T = 1$) and control ($T = 0$) populations and return the difference, known as T-learner Künzel et al. (2019) or “Two Models” Radcliffe & Surry (2011). A variation of this approach with larger model capacity have been proposed through a shared representation (SDR) for the treatment and control group in Betlei et al. (2018). Also, a prolific series

of work exists on adapting decision trees and random forests to the causal inference framework Athey & Imbens (2016); Wager & Athey (2018); Athey et al. (2019). Further in the same vein and building on work done on double machine learning by Chernozhukov et al. (2018), Oprescu et al. (2019) generalize the idea of causal forests, allowing for high-dimensional confounding. Finally, another recent trend is to study theoretical limits in ITE estimation and especially generalization bounds Shalit et al. (2017); Alaa & Van Der Schaar (2018).

Then regarding the concept of non compliance, many algorithms have been studied in order to recover (individual) causal effect in non-compliance settings, however to our knowledge, works tackling this problem focus solely on effect of the treatment intake M – and not the treatment prescription T – on the outcome Y (Gordon et al., 2019). In that context, the effect of T on Y is sometimes studied in an instrumental variable framework to recover the effect of M on Y Imbens & Angrist (1994); Syrgkanis et al. (2019). We focus in estimating the effect of the treatment prescription T on the variable Y , taking advantage of the observed treatment intake M , in the spirit of individual intention-to-treat (ITT) analysis (Montori & Guyatt, 2001; Gupta, 2011). The idea of taking advantage of a mediation variable to recover individual treatment effect has been explored notably by Hill et al. (2015), however the associated assumptions (M and Y are unconfounded) are more restrictive than the ones we propose, as we do not require the binary mediation variable M (representing the treatment intake) to be unconfounded with Y . We do however assume that it satisfies a strong monotonicity assumption with respect to the binary variable T , *i.e.* $T = 0 \Rightarrow M = 0$: an analogous assumption is referred to as *one-sided non-compliance* by Gordon et al. (2019). Similar monotonicity assumptions are typically made in causal inference works but concern the causal effect: the outcome Y is assumed to be monotonous with respect to the treatment T Kallus (2019); Oberst & Sontag (2019).

Finally, many research works validate their approach using synthetic data, in which a pointwise error measure named Precision Estimation of Heterogeneous Effect (PEHE) Shalit et al. (2017) can be computed. However in real world cases, the *fundamental problem of causal inference* states that the ground truth of individual treatment effect cannot be observed (since an individual is either treated or untreated but never both at the same time), preventing to use such metrics beyond simulation studies. Since our main motivation is to determine which individuals are good candidates for treatment prescription, we choose to evaluate the performance of our estimators on real data using the AUUC, which evaluates the ranking of individuals implied by corresponding ITE or IPE predictions. One can view the resulting measure as a prediction of the expected benefit of assigning treatment according to the model prediction instead of a random uniform prescription. Overall AUUC has been used in recent years in machine learning research to evaluate baseline ITE models vs SDR Diemert et al. (2018), flavors of Support Vector Machines for ITE estimation Kuusisto et al. (2014) or direct treatment policy optimization Yamane et al. (2018). For completeness a variant normalized by the ranking of an oracle model exists also under the name Qini coefficient Radcliffe & Surry (2011).

3 Framework

We briefly recall causality notions used throughout the paper, such as *structural causal model*, *causal graph*, *intervention* and *valid adjustment set* first introduced by Pearl (2009), and presented in Peters et al. (2017).

Definition 1 *Structural Causal Model (SCM)* A SCM of variables $\mathbf{X} = \{X_1, \dots, X_d\}$ is an object $\mathfrak{C} := (\mathbb{S}, \mathbb{P}_{\mathbf{N}})$ where:

- (1) \mathbb{S} is a set of d structural assignments $X_i = f_i(\mathbf{PA}_i, N_i)$, with the f_i 's deterministic functions and \mathbf{PA}_i the set of parents (direct causes) of X_i .
- (2) $\mathbb{P}_{\mathbf{N}} = \mathbb{P}_{N_1, \dots, N_d}$ is a joint distribution over the noise variables $\{N_i\}_{1 \leq d}$, which we require to be jointly independent.

As shown in Chapter 6 of Peters et al. (2017), a SCM \mathfrak{C} induces a unique *causal graph* $\mathcal{G}_{\mathfrak{C}}$, defined

as the directed acyclic graph (DAG) obtained by creating a vertex for each X_i and drawing directed edges from each \mathbf{PA}_i to X_i , thus justifying the term ‘parents’ for the sets \mathbf{PA}_i , and a unique *entailed distribution* $\mathbb{P}^{\mathfrak{C}}$ over variables X_1, \dots, X_d such that for each i , $X_i = f_i(\mathbf{PA}_i, N_i)$ in distribution.

A SCM can be used to define *interventional distributions*. A (hard) intervention $do(X_i = x_i)$ is a forced assignment of variable X_i to the value x_i , which implies a change in the distribution of the variables X_1, \dots, X_d . Formally, an intervention $do(X_i = x_i)$ is equivalent to modifying \mathfrak{C} in two ways: (1) change the structural assignment $X_i = f_i(X_i, \mathbf{PA}_i)$ to $X_i = x_i$ in \mathbb{S} and (2) replace X_i by x_i in all other structural assignments implying X_i in \mathbb{S} .

We will denote by $\mathbb{P}^{\mathfrak{C}; do(X_i := x_i)}$ the probability distribution entailed by the SCM \mathfrak{C} under the intervention $do(X_i := x_i)$.

Let $X_i, X_j \in \mathbf{X}$, $\mathbf{Z} \subseteq \mathbf{X} \setminus \{X_i, X_j\}$ is called a *valid adjustment set* (VAS) for the ordered pair (X_i, X_j) , if

$$\mathbb{P}^{\mathfrak{C}; do(X_i)}(X_j) = \sum_{\mathbf{z}} \mathbb{P}^{\mathfrak{C}}(X_j | X_i, \mathbf{z}) \mathbb{P}^{\mathfrak{C}}(\mathbf{z}),$$

where the sum is over the range of \mathbf{Z} .

Notations. For sake of compactness, we use the following notations for any binary variable W and multi-dimensional variable X : $\mathbb{P}(W) \triangleq \mathbb{P}(W = 1)$, $\mathbb{P}(\bar{W}) \triangleq \mathbb{P}(W = 0)$, $\mathbb{P}(x) \triangleq \mathbb{P}(X = x)$, $\mathbb{P}^{\mathfrak{C}; do(W)}(.) \triangleq \mathbb{P}^{\mathfrak{C}; do(W:=1)}(.)$.

3.1 Non-compliance setting

The setting of non-compliance we consider in this work is entirely defined by a SCM of variables X, T, M, Y, U for which example values were proposed in Table 1: X , belonging to a multi-dimensional space \mathcal{X} , contains the individual’s descriptive features (by simplicity, we will confuse the individual and their features, referring for example to ‘an individual x ’), T is the binary treatment prescription variable, M is the binary mediation variable, corresponding to the treatment acceptance, *i.e.* the fact that the individual did not interfere with their treatment prescription, Y is the binary outcome variable, U represents (allowed) unobserved confounders between X and Y .

In what follows, we define the structural causal model $\mathfrak{C} = (\mathbb{S}, \mathbb{P}_{\mathbf{N}})$, which is henceforth assumed to represent the causal mechanisms underlying the variables of interest in our work.

\mathbb{S} is defined in Equations 2:

$$\begin{aligned} T &= \tilde{N}_T \\ U &= N_U \\ X &= f_X(U, N_X) \\ M &= f_M(X, N_M) \times T \\ Y &= f_Y(X, M, U, N_Y). \end{aligned} \tag{2}$$

$\mathbb{P}_{\mathbf{N}}$ satisfies the following mild conditions: N_U, N_X, N_M, N_Y are noise consistent with variables definitions, and \tilde{N}_T is distributed according to a Bernoulli distribution with parameter $p = \mathbb{P}^{\mathfrak{C}}(T)$, consistent with a randomized controlled experiment setting.

The associated causal graph $\mathcal{G}_{\mathfrak{C}}$ is given in Figure 1

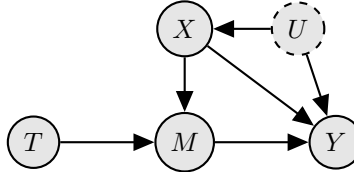


Figure 1: Causal graph $\mathcal{G}_{\mathfrak{C}}$ induced by the SCM \mathfrak{C}

In the next proposition, we list four assumptions implied by \mathfrak{C} about the variables of interest.

Proposition 1 *The SCM \mathfrak{C} defined in Equations 2 implies the following assumptions on variables T , M , Y and X :*

$$\begin{aligned}
& (\textit{Randomized treatment}) \quad T \perp\!\!\!\perp X \\
& (\textit{Exclusive treatment effect}) \quad T \perp\!\!\!\perp Y \mid \{X, M\} \\
& (\textit{One-sided non-compliance}) \quad T = 0 \Rightarrow M = 0 \\
& (\textit{Valid covariate adjustment}) \quad \{X\} \text{ is a VAS for } (M, Y)
\end{aligned} \tag{3}$$

The fact that \mathfrak{C} implies the *randomized treatment* and *Exclusive treatment effect* assumptions relies on the Markov property of the causal graph $\mathcal{G}_{\mathfrak{C}}$ and the notion of d-separation. The *One-sided non-compliance* is straightforwardly implied by the structural assignment of M given in Equations 2, while the *valid covariate adjustment* assumption relies on the back-door criterion (Pearl, 2009; Peters et al., 2017). The complete proof of Proposition 1, including definitions of the associated notions, is given in appendix.

Detailed review of assumptions. We now review in details the assumptions presented in Equation 3 and their connections to applications and usual theoretical settings.

- *Randomized treatment* translates the fact that each individual is randomly allocated to a treatment prescription ($T = 1$) or a control ($T = 0$) group, allowing us to infer the causal effect of T on Y without worrying about confounding bias. This is a typical situation in experiments such as A/B tests or randomized controlled clinical trials.
- *Exclusive treatment effect* captures the fact that the prescription to treatment T has an effect on the outcome Y only if the treatment is actually taken $M = 1$. More generally, this assumption translates the fact that the effect of T on Y is fully mediated by M . This is typically assumed to be the case in online advertising, in which case T is the allocation to treatment or control conditions and M is the actual exposure to advertisement Gordon et al. (2019).
- *One-sided non-compliance* (Gordon et al., 2019) states that $T = 0 \implies M = 0$, but that $T = 1 \not\Rightarrow M = 1$. In other words, treatment is only taken ($M = 1$) in cases where it was originally assigned ($T = 1$). This assumption is typically satisfied in the instrumental variable setting where T plays the role of the instrument for the estimation of the effect of M on Y (Syrkanis et al., 2019), the main difference with our work resides in the fact that we are interested in the effect of T on Y , IPE.
- *Valid covariate adjustment*: there is no confounder, outside of X , for the effect of M on Y . This assumption is classically made in ITE estimation works (Alaa & Van Der Schaar, 2018, 2019) and is sometimes referred to as *ignorability* Shalit et al. (2017). Under the potential outcome framework Rubin (2005), this assumption is equivalent to $Y(M = 1), Y(M = 0) \perp\!\!\!\perp M \mid X$. Strong ignorability (where we additionally assume that $0 < \mathbb{P}(M|x) < 1$ for all x) has been proven to be sufficient to recover the individual causal effect of M on Y (Imbens & Wooldridge, 2009; Pearl, 2017).

3.2 IPE in presence of non-compliance

Notations. For all $x \in \mathcal{X}$, we define the individual prescription effect $\tau^{IPE}(x)$, treatment effect if treated $\tau^{ITE}(x)$, as well as the individual compliance $\gamma(x)$ probability (that we henceforth refer to as *individual compliance* for clarity) as follows:

$$\begin{aligned}
\tau^{IPE}(x) &= \mathbb{P}^{\mathfrak{C}; do(T)}(Y|x) - \mathbb{P}^{\mathfrak{C}; do(\overline{T})}(Y|x), \\
\tau^{ITE}(x) &= \mathbb{P}^{\mathfrak{C}; do(M)}(Y|x) - \mathbb{P}^{\mathfrak{C}; do(\overline{M})}(Y|x), \\
\gamma(x) &= \mathbb{P}^{\mathfrak{C}; do(T)}(M|x).
\end{aligned} \tag{4}$$

We also define the relative ITE $\beta(x)$ and relative IPE $\alpha(x)$ as:

$$\alpha(x) = \frac{\mathbb{P}^{\mathfrak{C}}(Y|T, x) - \mathbb{P}^{\mathfrak{C}}(Y|\overline{T}, x)}{\mathbb{P}^{\mathfrak{C}}(Y|\overline{T}, x)}$$

$$\beta(x) = \frac{\mathbb{P}^{\mathfrak{C}}(Y|M, x) - \mathbb{P}^{\mathfrak{C}}(Y|\overline{M}, x)}{\mathbb{P}^{\mathfrak{C}}(Y|\overline{M}, x)}.$$

The proposed method exploits the mediation variable M , *i.e.* the treatment acceptance, by splitting the treatment to outcome path into a product of two *subpaths*, both with a higher signal-to-noise ratio. In particular, under \mathfrak{C} , we can integrate M into the $\mathbb{P}^{\mathfrak{C};do(T)}(Y|x)$ expression as presented in the next lemma.

Lemma 1 *Assuming \mathfrak{C} , and for any $x \in \mathcal{X}$, the positive outcome probability under treatment, $\mathbb{P}^{\mathfrak{C};do(T)}(Y|x)$, can be written as follows:*

$$\mathbb{P}^{\mathfrak{C};do(T)}(Y|x) = \mathbb{P}^{\mathfrak{C}}(Y|x, \overline{M}) + \mathbb{P}^{\mathfrak{C}}(M|x, T) \left(\mathbb{P}^{\mathfrak{C}}(Y|x, M) - \mathbb{P}^{\mathfrak{C}}(Y|x, \overline{M}) \right). \quad (5)$$

The proof of Lemma 1 is fully detailed on appendix. It relies on *valid covariate adjustment*, *randomized treatment*, and *exclusive mediation* assumptions, that we have proven to be implied by \mathfrak{C} in Proposition 1.

The different terms of Equation (5) have an intuitive interpretation, indeed:

$\mathbb{P}^{\mathfrak{C}}(M|x, T) = \gamma(x)$ is the compliance of individual x , *i.e.* the probability an individual with features x who is assigned to treatment accepts this treatment. $\mathbb{P}^{\mathfrak{C}}(Y|x, M) - \mathbb{P}^{\mathfrak{C}}(Y|x, \overline{M}) = \tau^{ITE}(x)$ is the ITE of user x . $\mathbb{P}^{\mathfrak{C}}(Y|x, \overline{M})$, the individual probability of positive outcome of an individual x given they did not receive treatment. It is referred to as the *organic* probability of positive outcome.

In a nutshell, the Lemma 1 decomposes the positive outcome probability under treatment of a given individual as the sum of the organic positive outcome probability and the product of individual compliance and individual treatment effect if treated.

In Proposition 2, we present a result linking the IPE, the ITE and the individual compliance:

Proposition 2 *Assuming \mathfrak{C} , the IPE decomposes as follows:*

$$\tau^{IPE}(x) = \tau^{ITE}(x)\gamma(x) \quad (6)$$

The proof of Proposition 2 is fully detailed in appendix. It relies on the identity $\mathbb{P}^{\mathfrak{C};do(\overline{T})}(Y|x) = \mathbb{P}^{\mathfrak{C}}(Y|x, \overline{M})$, which holds under \mathfrak{C} thanks to the *exclusive mediation* and *strong mediation monotonicity* assumptions.

In intuitive terms, the individual prescription effect (IPE) is expressed as the individual treatment effect (ITE) multiplied by the individual compliance probability.

4 Proposed Approach

4.1 Definition and basic properties

The expression proven in Proposition 2 calls for a novel way to estimate individual treatment effect, by first estimating separately both factors $\tau^{ITE}(x)$ and $\gamma(x)$, then multiplying these estimators to form a *compliance aware individual intention-to-treat effect* (C-IPE) estimator.

Formally, let $\hat{\tau}^{ITE}$ be an estimator of τ^{ITE} , let $\hat{\gamma}$ be an estimator of γ . We then define the associated C-IPE estimator $\hat{\tau}^{C-IPE}$, for any x , as:

$$\hat{\tau}^{C-IPE}(x) = \hat{\tau}^{ITE}(x)\hat{\gamma}(x). \quad (7)$$

In practice, $\hat{\tau}^{ITE}$ may be obtained using any individual treatment effect estimator. Indeed, under \mathfrak{C} , the individual causal effect of M on Y given X is recoverable since $\{X\}$ is a valid adjustment set for

(M, Y) as explained in Section 3. C-IPE is not an estimator per say, but rather a meta-estimator: a black-box in which any classical ITE and compliance estimators can be plugged-in.

Assuming that x , $\hat{\tau}^{ITE}(x)$ and $\hat{\gamma}(x)$ are *consistent* estimators of resp. $\tau^{ITE}(x)$ and $\gamma(x)$, Proposition 2 then ensures that $\hat{\tau}^{C-IPE}(x)$ is a *consistent* estimator of $\tau^{IPE}(x)$.

4.2 Asymptotic variance properties

Thanks to its expression as a function of a ITE estimator, the C-IPE estimator *focuses* on the individuals who actually accepted treatment, who we know to be the only individuals contributing to the IPE signal (*Exclusive treatment effect* assumption in Equation 3). We therefore expect the C-IPE estimator to have lower variance than an IPE estimator which does not exploit the observable compliance. Comparing a C-IPE and an IPE estimator is all the more fair than we use an analogous version of the ITE estimator for the ITE estimator the C-IPE estimator is built on, which we know to be feasible thanks to the *valid covariate adjustment* assumption. We refer to this approach as *symmetrically learning algorithms comparison*, and use it to conduct our experiments in Section 5.

In the following proposition, we compare the asymptotic variance of estimators $\hat{\tau}^{C-IPE}$ and $\hat{\tau}^{IPE}$ in the following simple yet realistic setting:

Single-stratum setting. We focus on the IPE estimation for a single value x_0 of X , for which we assume to observe n *i.i.d.* samples $\{(x_0, T_i, M_i, Y_i)\}_{1 \leq i \leq n}$. In practice, this generalises to any stratum $S \subset \mathcal{X}$ containing x_0 for which the adjustment set formula is valid, *i.e.* if the variable $X' \triangleq x_0 I_{X \in S} + X I_{X \notin S}$ defines a valid adjustment set for (M, Y) .

Notations. Consistently with notations presented in Equations 4, $\alpha(x_0)$, $\beta(x_0)$ refer respectively to the relative IPE and relative ITE in stratum $\{X = x_0\}$ (and are assumed to be positive in this illustrative setting), and we denote $\hat{\gamma}(x_0)$, $\hat{\tau}^{IPE}(x_0)$ and $\hat{\tau}^{ITE}(x_0)$ respectively the maximum-likelihood estimator (MLE) of $\gamma(x_0)$, and the MLE-based two-model estimators (difference of two MLE estimators) of $\tau^{IPE}(x_0)$ and $\tau^{ITE}(x_0)$. We define the associated C-IPE estimator as $\hat{\tau}^{C-IPE}(x_0) \triangleq \hat{\gamma}(x_0)\hat{\tau}^{ITE}(x_0)$. Lastly, we denote $p_1(x_0) = \mathbb{P}^{\mathfrak{C}}(Y|T, x_0)$.

In the following Proposition, we present an asymptotic bound for the ratio of the standard deviation (*sd*) of C-IPE and IPE estimators.

Proposition 3 *Under \mathfrak{C} defined in Section 3.1 with $\mathbb{P}^{\mathfrak{C}}(T) = \frac{1}{2}$, assuming we observe n *i.i.d.* samples in stratum $\{X = x_0\}$, we have:*

$$\lim_{n \rightarrow \infty} \frac{sd(\hat{\tau}^{C-IPE})}{sd(\hat{\tau}^{IPE})} \leq \sqrt{\left(\frac{2(1 + \beta)}{(1 - p_1)(2 + \alpha)} \right) \gamma} \quad (8)$$

where we dropped the reference to x_0 for clarity.

This theoretical bound shows that the ratio of standard deviations of C-IPE and IPE estimators is smaller as the compliance factor $\gamma(x_0)$ decreases. However, additional assumptions need to be made about $\beta(x_0)$ and $p_1(x_0)$ in order to recover an informative bound in practice.

In real-world datasets presented in Section 5, we consistently observe $\hat{\beta}(x) \leq 12$ and $\hat{p}_1(x) \leq 0.05$, where the estimators correspond to logistic regression models fined-tuned following the protocol described in Section 5. Under such assumptions on the orders of magnitude of $\beta(x_0)$ and $p_1(x_0)$, we can derive a useful-in-practice bound, as presented in the following remark.

Remark 1 *If we additionally assume $\beta(x_0) \leq 12$, and $p_1(x_0) \leq 0.05$ we have:*

$$\lim_{n \rightarrow \infty} \frac{sd(\hat{\tau}^{C-IPE})}{sd(\hat{\tau}^{IPE})} \leq 4\sqrt{\gamma}. \quad (9)$$

This bound is derived from loose upper-bounds on $\beta(x_0)$ and p_1 and is only presented for illustrative purposes. It is however still informative in case of low compliance probability (low $\gamma(x_0)$). For instance, with $\gamma(x_0) \leq 10^{-2}$, Equation 9 reveals that the asymptotic standard deviation of $\hat{\tau}^{C-IPE}$ is more than twice smaller than the one of $\hat{\tau}^{IPE}$.

5 Experiments

To qualify the performance of the C-IPE estimator, we study its benefits in a variety of settings. Firstly we study its properties on simulation-based studies, hereafter denoted by ‘Synthetic Datasets’, for which i) the IPE ground truth is known ii) the level of compliance can be controlled and iii) we can appreciate performance with respect to an Oracle. Moreover we apply our approach to transform baseline IPE estimators and compare their performance on real-world, large scale datasets, for which we shall recover the AUUC. The first one is an open dataset from Criteo, named ‘CRITEO-UPLIFT1 Dataset’¹. Finally we have privileged access on two other *private* datasets, designated by ‘Private datasets’.

In each experiment we take care of comparing symmetrically learning algorithms for which we provide or not the C-IPE estimator decomposition so as to highlight corresponding benefits or drawbacks. To simplify experiments we chose two base models: Two Models (2M) and SDR as they easily scale to large datasets and have been found competitive in prior studies Betlei et al. (2018). For reproducibility sake we have implemented models using Scikit-Learn Python library Pedregosa et al. (2011) (code provided as supplementary). All experiments were run on a machine with 48 CPUs (Intel(R) Xeon(R) Gold 6146 CPU @ 3.20GHz), with 2 Threads per core, and 500Go of RAM. Finally, we note that the state of the art is always evolving and improving. We did not use the most advanced models because we do not aim at outperforming them. Instead, we claim that the C-IPE estimator can improve any IPE estimator (while keeping the same individual treatment effect model) in the case of low observable compliance.

5.1 Datasets

Synthetic Datasets

We define a simulation setting in which $\mathcal{X} = \{0, 1\}^{10}$, $N = 2.10^6$. The response is generated according to

$$Y \sim \text{Bern}(p_0(1 + TM\beta(x))), \quad (10)$$

where $T \sim \text{Bern}(0.5)$, $M \sim \text{Bern}(\gamma(x))$, and $p_0 = \mathbb{P}^c(Y|\overline{M}, x) = 0.1$, using notations from Equations 4. This procedure allows for varying $\gamma(x)$ and $\beta(x)$ to simulate different levels of compliance and relative ITE, respectively.

CRITEO-UPLIFT1 Dataset

We use the CRITEO-UPLIFT1 dataset where data were collected using a randomized trial, from an advertising application. Key statistics for this dataset are summarized in Table 2 and 3. Notably, average treatment prescription $\mathbb{E}[T] \approx .85$ indicates that only about 15% of users were assigned to the control group (without any advertisement). The advertisers participated in online ad auctions for the rest of the population. Among the users that advertisers tried to expose ($T = 1$), only 3.65% were actually exposed, which is an extremely low compliance level, expected to highlight C-IPE estimator benefits. Effective exposure to ads embodies the M variable in this setup. Treatment prescription and compliance rates are illustrated on Figure 2. The outcome of interest Y is the variable ‘user visiting the advertiser website’, and its mean is more than 10x higher given actual exposure ($M = 1$) versus non-exposure ($M = 0$).

Private Datasets

We have access to two private datasets of 90M instances, which contain binary treatment and outcome, and a suitable variable that embodies an observable compliance. They have a higher compliance γ (7.8% and 10.4%), higher number of features (48) and similar signal strength than the CRITEO-UPLIFT1

¹<http://cail.criteo.com/criteo-uplift-prediction-dataset/>

Table 2: Distribution of users effectively treated ($M = 1$) and visits ($Y = 1$) on CRITEO-UPLIFT1 split on treatment groups

TREATMENT (T)	EXPOSURE (M)	OUTCOME (Y)
0 (2'096'236)	-	3.82% (79'986)
1 (12'161'477)	3.65% (444'384)	4.93% (599'170)

Table 3: Repartition of visits ($Y = 1$) on CRITEO-UPLIFT1 split on exposure groups

EXPOSURE (M)	OUTCOME (Y)
0 (13'813'329)	3.58% (495'003)
1 (444'384)	41.4% (184'153)

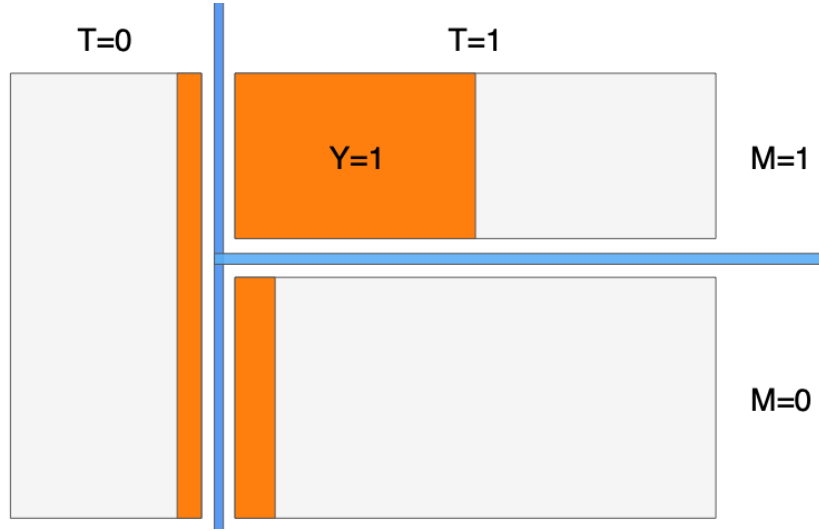


Figure 2: The visit users repartition is mainly influenced by the mediation variable M on the CRITEO-UPLIFT1 dataset

dataset. The purpose of extending the study to these datasets is to verify the relationship between compliance level and performance, predicted by the theoretical study in Section 4.2. The corresponding data has been collected in the same geographical location, during two separate time periods).

5.2 Experiments

A common procedure for all experiments is to select hyperparameters (regularization norm and strength) of models using internal cross validation on the training set. For the C-IPE estimators we recall that an additional probabilistic model of the compliance $\hat{\gamma}(x)$ is required. For all experiments it is learned on the training data as a logistic regression. Hyperparameters are selected by internal cross-validation on the training set by ranking by log-likelihood (LLH) as the model is supposed to predict a probability.

Compliance Sensitivity Experiment (Simulation)

The goal is to highlight how the compliance level γ influences the performance of both the traditional IPE estimator and C-IPE estimator. For this purpose we vary $\gamma \in [10^{-4}; .99]$ and generate synthetic datasets as described in Section 5.1 with a different value β (in $\{-1, 0, 1, 2, 3, 4, 5, 6, 7, 8\}$) for each of the 10 contexts. We report the PEHE metric for both estimators and estimate variance by repeating experiment with 51 random test/train splits. Recall that PEHE is the squared difference between the IPE ground truth and the prediction of the model.

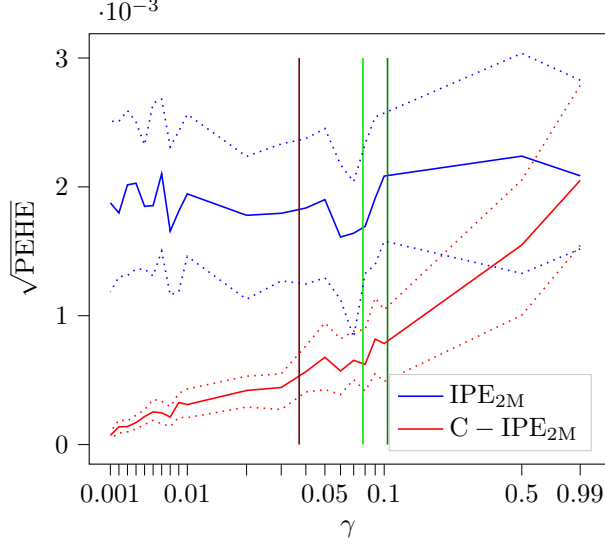


Figure 3: **Compliance Sensitivity (Simulation study)**. PEHE (lower is better) of IPE vs C-IPE models at varying compliance level γ . Solid line — represents the median, and dashed line represents 5% and 95% of confidence intervals. —, — and —: compliance level γ for resp. CRITEO-UPLIFT1 and private datasets 1 & 2. The x-axis has a simlog scale.

We observe on Figure 3 that the C-IPE estimator significantly outperforms the IPE estimator when the level of compliance is low (low γ) and has similar performance to baseline IPE when there is full compliance (γ close to 1). This shows that our post-mediation approach significantly reduces the noises due to non-compliance and can learn a smaller signal. This is true in particular for compliance levels γ in the range that is observed on real datasets.

Baseline Experiment (Simulation)

For the synthetic dataset, the goal is to simulate a realistic scenario where there exists heterogeneity in compliance and post-mediation treatment effects. More precisely, for each instance value x , we draw once and for all $\gamma \in \{0.01, 0.005\}$ and $\beta \in \{-1, 1, 3, 5, 7\}$ uniformly and independently. Associated outcome is computed according to the synthetic dataset equation (10). We study four methods: regular two-models (IPE_{2M}), shared data representation (IPE_{SDR}) and their variants, obtained by adding the intermediate variable M (resp. $\text{C} - \text{IPE}_{2M}$, and $\text{C} - \text{IPE}_{\text{SDR}}$). We focus on AUUC metric because real-world application cannot access individual treatment effect ground truth. Recall that AUUC measures the capacity of the model to rank individuals according to their IPE. In order to make sure that learned models perform better than random, we subtract the AUUC of a random model, obtaining ΔAUUC . Finally to scale the performance of the latter models, we report in Figure 4 results for an Oracle model that has access to the drawn (β, γ) , and for IPE_{best} , the best possible learnt model without exploiting the observable compliance M (it predicts for each x its empirical IPE average based

on the training set). Again, variance is estimated by repeating experiment with 51 random test/train splits.

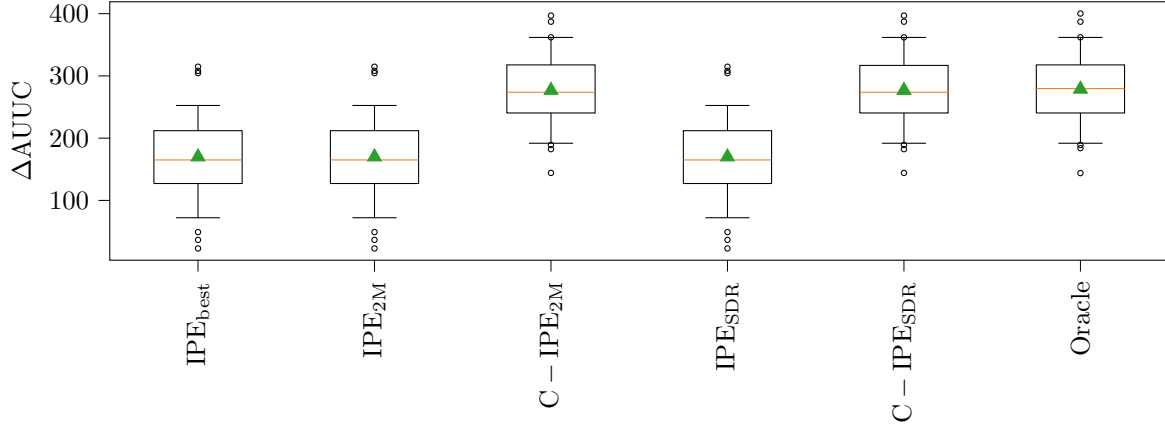


Figure 4: **Baseline Experiment (Simulation).** $\Delta AUUC$ (higher is better) of two IPE models, corresponding C-IPE models and Oracle model (theoretical truth). Box plots are done on 51 random splits, whiskers at 5/95 percentiles. Note how C-IPE systematically increases AUUC of base estimators.

Figure 4 assesses the performance of C-IPE estimators versus IPE, using the $\Delta AUUC$ metric. They yield a higher $\Delta AUUC$ in more than 90% of the random splits. Moreover C-IPE estimators are close to the Oracle (best model possible) as the Oracle does not significantly outperform them, note that even the Oracle can misrank users because the validation set is noisy and empirical IPEs do not always follow the expected ranking. Besides, Figure 4 does not show any limitation of the 2M and SDR models, but rather highlight the ineffectiveness of such direct IPE estimators if a low compliance is observed. This phenomenon can be improved by our post-mediation approach thanks to the higher signal of the causal effect of M on Y . Of course, this synthetic data encodes a simpler setting than real-world data, but the fact that our proposed post-mediation approach performs that high still confirms our theoretical analysis.

Real-world Experiment (CRITEO-UPLIFT1)

To qualify the benefit of C-IPE versus IPE for real-world applications we report $\Delta AUUC$ on the CRITEO-UPLIFT1 dataset. We study four methods: two IPE models (IPE_{2M} , and IPE_{SDR}) and their C-IPE variants (resp. $C - IPE_{2M}$, and $C - IPE_{SDR}$). For the additional $\hat{\gamma}(x)$ model, care is taken to weight the LLH as there is a high imbalance between $M = 1$ and $M = 0$ classes. We use as an hyper-parameter grid the Cartesian product of $\{L1, L2\}$ (regularization) and $\{0.01, 1, 10^2, 10^5\}$ (C , inverse of regularization strength) for $\hat{\gamma}(x)$. Best hyper-parameters found are L1 regularization and $C = 100$. Results are presented on Figure 5.

The C-IPE version of each models reduces the variance of the $\Delta AUUC$ estimate. This was expected and somehow justified in Proposition 3. Moreover, although the confidence intervals are slightly superposed, C-IPE always outperforms its IPE counterpart on the 51 splits.

Real-world Experiment (Private Datasets)

For the private datasets, we repeat the same procedure and compare the same metrics. Figure 6 illustrates the differences in $\Delta AUUC$ of the learned models and a random model on 33 bootstraps. The C-IPE models performs better than the two IPE models by having an AUUC significantly better than the random model, when the two IPE models do not perform better than the random model.

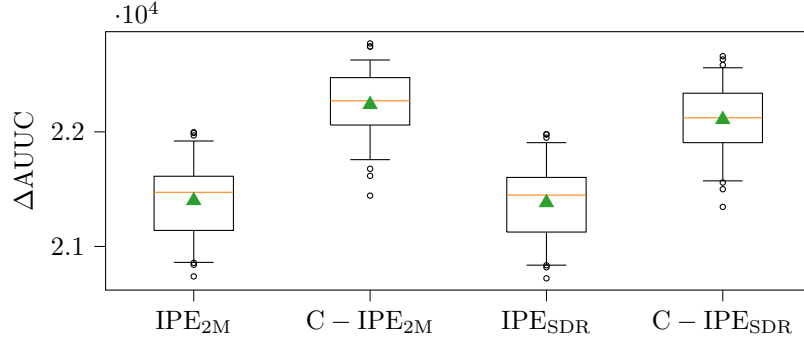


Figure 5: **Real-world Experiment (CRITEO-UPLIFT1)**. $\Delta AUUC$ (higher is better) on test for two IPE models and corresponding C-IPE models. Box plots computed on 51 random splits, whiskers at 5/95 percentiles. Note the higher $\Delta AUUC$ and reduced variance of C-IPE models.

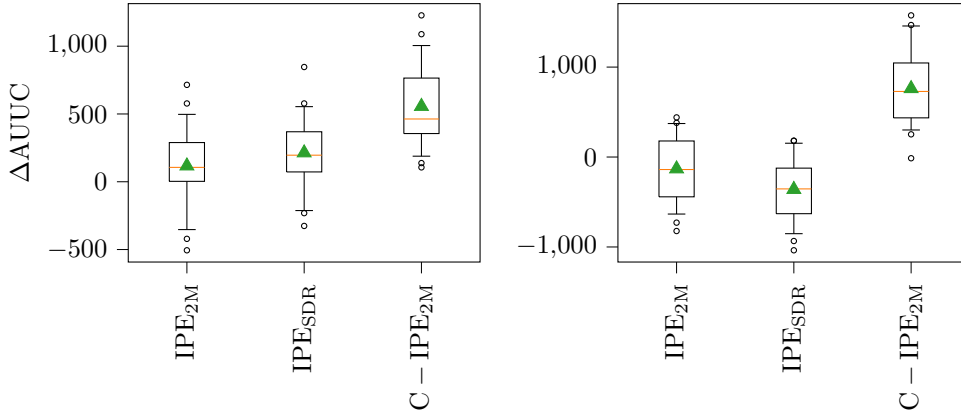


Figure 6: **Real-world Experiment (Private Datasets)**. AUUC (higher is better) of two IPE models and one C-IPE model (based on two models) from which we subtracted the AUUC of a random model. Box plots are done on 33 bootstraps, whiskers at 5/95 percentiles.

An interesting finding of this experiment is that, in practice, the mild expected benefit of C-IPE, predicted by the theory (because of a higher compliance than in CRITEO-UPLIFT1 dataset) does not seem discernible. This is however only an indication as there are multiple differences between the two datasets that might explain such a behavior.

6 Conclusion and Future Works

We propose a novel approach on individual prescription effect (IPE) estimation exploiting observed compliance to the treatment prescription.

Using the structural causal model framework, we define assumptions under which the IPE can be expressed as a product of the individual treatment effect (ITE) and the individual level of compliance. In this setting, our post-mediation individual treatment effect (C-IPE) estimator is consistent. Moreover its asymptotic variance improves with the level of compliance. Experimentally, we show how the performance of several baseline IPE estimators improve when plugged in the C-IPE meta-estimator. We also observe the relationship between performance and compliance as predicted by our theoretical results.

Finally, this work opens several perspectives among which: i) stability of our results under variations of assumptions, ii) bound tightness and properties in high-dimensional contexts, and iii) exploration of how representation learning approaches may uncover by themselves C-IPE-like estimator decomposition under weaker causal assumptions.

References

- Alaa, A. and Van Der Schaar, M. Limits of estimating heterogeneous treatment effects: Guidelines for practical algorithm design. In *Proceedings of the International Conference on Machine Learning*, 2018.
- Alaa, A. and Van Der Schaar, M. Validating causal inference models via influence functions. In *Proceedings of the International Conference on Machine Learning*, 2019.
- Athey, S. and Imbens, G. Recursive partitioning for heterogeneous causal effects. *Proceedings of the National Academy of Sciences*, 113(27), 2016.
- Athey, S., Tibshirani, J., Wager, S., et al. Generalized random forests. *The Annals of Statistics*, 47(2), 2019.
- Betlei, A., Diemert, E., and Amini, M.-R. Uplift prediction with dependent feature representation in imbalanced treatment and control conditions. In *Proceedings of the International Conference on Neural Information Processing*, 2018.
- Chernozhukov, V., Chetverikov, D., Demirer, M., Duflo, E., Hansen, C., Newey, W., and Robins, J. Double/debiased machine learning for treatment and structural parameters. *The Econometrics Journal*, 2018.
- Devriendt, F., Moldovan, D., and Verbeke, W. A literature survey and experimental evaluation of the state-of-the-art in uplift modeling: A stepping stone toward the development of prescriptive analytics. *Big data*, 6(1), 2018.
- Diemert, E., Betlei, A., Renaudin, C., and Amini, M.-R. A large scale benchmark for uplift modeling. In *Proceedings of the AdKDD and TargetAd Workshop*, 2018.
- Foster, J. C., Taylor, J. M., and Ruberg, S. J. Subgroup identification from randomized clinical trial data. *Statistics in medicine*, 30(24), 2011.
- Gordon, B. R., Zettelmeyer, F., Bhargava, N., and Chapsky, D. A comparison of approaches to advertising measurement: Evidence from big field experiments at facebook. *Marketing Science*, 38(2), 2019.
- Gupta, S. K. Intention-to-treat concept: a review. *Perspectives in clinical research*, 2(3):109, 2011.
- Hill, D. N., Moakler, R., Hubbard, A. E., Tsemekhman, V., Provost, F., and Tsemekhman, K. Measuring causal impact of online actions via natural experiments: Application to display advertising. In *Proceedings of the International Conference on Knowledge Discovery and Data Mining*, 2015.
- Imbens, G. W. and Angrist, J. D. Identification and estimation of local average treatment effects. *Econometrica*, 1994.
- Imbens, G. W. and Wooldridge, J. M. Recent developments in the econometrics of program evaluation. *Journal of economic literature*, 47(1), 2009.
- Jacob, D., Härdle, W. K., and Lessmann, S. Group average treatment effects for observational studies. *arXiv preprint arXiv:1911.02688*, 2019.
- Jin, J., Sklar, G. E., Oh, V. M. S., and Li, S. C. Factors affecting therapeutic compliance: A review from the patients perspective. *Therapeutics and clinical risk management*, 4(1):269, 2008.
- Kallus, N. Classifying treatment responders under causal effect monotonicity. *arXiv preprint arXiv:1902.05482*, 2019.

- Künzel, S. R., Sekhon, J. S., Bickel, P. J., and Yu, B. Metalearners for estimating heterogeneous treatment effects using machine learning. *Proceedings of the National Academy of Sciences*, 116(10), 2019.
- Kuusisto, F., Costa, V. S., Nassif, H., Burnside, E., Page, D., and Shavlik, J. Support vector machines for differential prediction. In *Joint European Conference on Machine Learning and Knowledge Discovery in Databases*, 2014.
- Montori, V. M. and Guyatt, G. H. Intention-to-treat principle. *Cmaj*, 165(10):1339–1341, 2001.
- Oberst, M. and Sontag, D. Counterfactual off-policy evaluation with gumbel-max structural causal models. *arXiv preprint arXiv:1905.05824*, 2019.
- Oprescu, M., Syrgkanis, V., and Wu, Z. S. Orthogonal random forest for causal inference. In *Proceedings of the International Conference on Machine Learning*, 2019.
- Parker, C. *Reducing the risk of policy failure: challenges for regulatory compliance: final version*. OECD, 2000.
- Pearl, J. *Causality*. Cambridge university press, 2009.
- Pearl, J. Detecting latent heterogeneity. *Sociological Methods & Research*, 46(3), 2017.
- Pedregosa, F., Varoquaux, G., Gramfort, A., Michel, V., Thirion, B., Grisel, O., Blondel, M., Prettenhofer, P., Weiss, R., Dubourg, V., et al. Scikit-learn: Machine learning in python. *Journal of machine learning research*, 12, 2011.
- Peters, J., Janzing, D., and Schölkopf, B. *Elements of causal inference: foundations and learning algorithms*. MIT press, 2017.
- Radcliffe, N. J. and Surry, P. D. Real-world uplift modelling with significance-based uplift trees. *Stochastic Solutions*, 2011.
- Rubin, D. B. Causal inference using potential outcomes: Design, modeling, decisions. *Journal of the American Statistical Association*, 100(469), 2005.
- Rzepakowski, P. and Jaroszewicz, S. Decision trees for uplift modeling. In *Proceeding of the International Conference on Data Mining*. IEEE, 2010.
- Rzepakowski, P. and Jaroszewicz, S. Decision trees for uplift modeling with single and multiple treatments. *Knowledge and Information Systems*, 32(2), 2012.
- Shalit, U., Johansson, F. D., and Sontag, D. Estimating individual treatment effect: generalization bounds and algorithms. In *Proceedings of the International Conference on Machine Learning*, 2017.
- Syrgkanis, V., Lei, V., Oprescu, M., Hei, M., Battocchi, K., and Lewis, G. Machine learning estimation of heterogeneous treatment effects with instruments. In *Proceedings of Advances in Neural Information Processing Systems*, 2019.
- Wager, S. and Athey, S. Estimation and inference of heterogeneous treatment effects using random forests. *Journal of the American Statistical Association*, 113(523), 2018.
- Xie, Y., Brand, J. E., and Jann, B. Estimating heterogeneous treatment effects with observational data. *Sociological methodology*, 42(1), 2012.
- Yamane, I., Yger, F., Atif, J., and Sugiyama, M. Uplift modeling from separate labels. In *Proceedings of Advances in Neural Information Processing Systems*, 2018.

A Proofs

To ensure a comfortable appendix read we quickly remind, for each lemma and proposition, vocabulary and notations introduced in the paper that are used in the associated proofs.

A.1 Proposition 1

The structural causal model $\mathfrak{C} = (\mathbb{S}, \mathbb{P}_{\mathbf{N}})$ is assumed to represent the causal mechanisms underlying the variables of interest in our work.

\mathbb{S} is defined in Equations (2), and $\mathbb{P}_{\mathbf{N}}$ satisfies the following mild conditions: N_U, N_X, N_M, N_Y are noise consistent with variables definitions, and \tilde{N}_T is distributed according to a Bernoulli distribution with parameter $p = \mathbb{P}^{\mathfrak{C}}(T)$, consistent with a randomized controlled experiment setting.

In Proposition 1, we list four assumptions implied by the \mathfrak{C} about the variables of interest.

Proof.

The proof of Proposition 1 relies on the notions of valid adjustment set (definition 6.38 of Peters et al. (2017)), its relation to the back-door criterion (Proposition 6.41 of Peters et al. (2017)), the notion of d-separation (Definition 6.1 of Peters et al. (2017)) and the Markov property (Proposition 6.21 of Peters et al. (2017)).

First of all, the SCM \mathfrak{C} is Markovian with respect to its own entailed distribution (Proposition 6.31 of Peters et al. (2017)): this implies that every conditional independence encoded (as a d-separation) in the graph $\mathcal{G}_{\mathfrak{C}}$ holds in distribution $\mathbb{P}^{\mathfrak{C}}$.

Randomized treatment, is implied by the Markov property and the fact that T and X are d-separated by the empty set in $\mathcal{G}_{\mathfrak{C}}$: all paths between T and X contain either $\rightarrow M \leftarrow$ or $\rightarrow Y \leftarrow$, which are blocked by not including neither M nor Y .

Exclusive treatment effect is implied by the Markov property and the fact that the set $\{X, M\}$ d-separates T and Y in $\mathcal{G}_{\mathfrak{C}}$. This is shown by listing all paths between T and Y and observing that they are all blocked by the set $\{X, M\}$.

One-sided non-compliance is straightforwardly implied by the structural assignment of M given in Equations (2).

Valid covariate adjustment relies on the back-door criterion for valid adjustment sets. We remark that $\{X\}$ satisfies the back-door criterion for (M, Y) because (i) it is not a descendant of M and (ii) it blocks all paths from M to Y that enter Y through the backdoor: it is therefore a valid adjustment set for the ordered pair (M, Y) . ■

A.2 Lemma 1

The proposed method exploits the mediation variable M , *i.e.* the treatment acceptance, by splitting the treatment to outcome path into a product of two *subpaths*, both with a higher noise-to-signal ratio. In particular, based on the causal graphical model 1, we can integrate M into the $\mathbb{P}^{\mathfrak{C}; do(T)}(Y|x)$ as presented in Lemma 1.

Proof.

Assuming the SCM \mathfrak{C} truly describes the relationships between T, X, M, Y , we have:

$$\begin{aligned}
\mathbb{P}^{\mathfrak{C};do(T)}(Y|x) &= \mathbb{P}^{\mathfrak{C};do(T)}(Y, M|x) + \mathbb{P}^{\mathfrak{C};do(T)}(Y, \overline{M}|x) \\
&= \underbrace{\mathbb{P}^{\mathfrak{C};do(T)}(Y|x, M)}_{\mathbb{P}^{\mathfrak{C}}(Y|x, M)} \mathbb{P}^{\mathfrak{C};do(T)}(M|x) + \underbrace{\mathbb{P}^{\mathfrak{C};do(T)}(Y|x, \overline{M})}_{\mathbb{P}^{\mathfrak{C}}(Y|x, \overline{M})} \mathbb{P}^{\mathfrak{C};do(T)}(\overline{M}|x) \\
&= \mathbb{P}^{\mathfrak{C}}(Y|x, M) \mathbb{P}^{\mathfrak{C};do(T)}(M|x) + \mathbb{P}^{\mathfrak{C}}(Y|x, \overline{M}) \mathbb{P}^{\mathfrak{C};do(T)}(\overline{M}|x) \\
&= \mathbb{P}^{\mathfrak{C}}(Y|x, M) \mathbb{P}^{\mathfrak{C};do(T)}(M|x) + \mathbb{P}^{\mathfrak{C}}(Y|x, \overline{M}) \underbrace{\mathbb{P}^{\mathfrak{C};do(T)}(\overline{M}|x)}_{1 - \mathbb{P}^{\mathfrak{C};do(T)}(M|x)} \\
&= \mathbb{P}^{\mathfrak{C}}(M|x, T) \left(\mathbb{P}^{\mathfrak{C}}(Y|x, M) - \mathbb{P}^{\mathfrak{C}}(Y|x, \overline{M}) \right) + \mathbb{P}^{\mathfrak{C}}(Y|x, \overline{M}),
\end{aligned}$$

where we used assumptions described Equation 3, namely:

- $\mathbb{P}^{\mathfrak{C};do(M)}(Y|x) = \mathbb{P}^{\mathfrak{C}}(Y|M, x)$ (*Valid covariate adjustment*),
- $\mathbb{P}^{\mathfrak{C};do(T)}(\cdot|x, \cdot) = \mathbb{P}^{\mathfrak{C}}(\cdot|x, T, \cdot)$ (*Randomized treatment*),
- $\mathbb{P}^{\mathfrak{C}}(Y|x, T, M) = \mathbb{P}^{\mathfrak{C}}(Y|x, M)$ (*Exclusive treatment effect*),

and the claim follows. ■

A.3 Proposition 2

For all $x \in \mathcal{X}$, we define the individual treatment effect $\tau^{IPE}(x)$, treatment effect if treated $\tau^{ITE}(x)$, as well as the individual compliance $\gamma(x)$ probability (that we henceforth refer to as *individual compliance* for clarity) in Equations (4).

In Proposition 2, we propose a result linking the IPE, the ITE and the compliance probability, namely

$$\tau^{IPE}(x) = \tau^{ITE}(x) \gamma(x).$$

Proof

We have an analogous version of (5) for the term $\mathbb{P}^{\mathfrak{C};do(\overline{T})}(Y|x)$:

$$\mathbb{P}^{\mathfrak{C};do(\overline{T})}(Y|x) = \mathbb{P}^{\mathfrak{C}}(Y|x, \overline{M}) + \mathbb{P}^{\mathfrak{C}}(M|x, \overline{T}) \left(\mathbb{P}^{\mathfrak{C}}(Y|x, M) - \mathbb{P}^{\mathfrak{C}}(Y|x, \overline{M}) \right).$$

Since $\overline{T} \Rightarrow \overline{M}$ (*One-sided non-compliance* assumption), we get that, $\forall x \in \mathcal{X}$, $\mathbb{P}^{\mathfrak{C}}(M|x, \overline{T}) = 0$, and finally:

$$\mathbb{P}^{\mathfrak{C};do(\overline{T})}(Y|x) = \mathbb{P}^{\mathfrak{C}}(Y|x, \overline{M}).$$

Then:

$$\begin{aligned}
\tau^{IPE}(x) &= \mathbb{P}^{\mathfrak{C};do(T)}(Y|x) - \mathbb{P}^{\mathfrak{C};do(\overline{T})}(Y|x) \\
&= \mathbb{P}^{\mathfrak{C}}(M|x, T) \left(\mathbb{P}^{\mathfrak{C}}(Y|x, M) - \mathbb{P}^{\mathfrak{C}}(Y|x, \overline{M}) \right) + \underbrace{\mathbb{P}^{\mathfrak{C}}(Y|x, \overline{M}) - \mathbb{P}^{\mathfrak{C}}(Y|x, \overline{T})}_{\mathbb{P}^{\mathfrak{C}}(Y|x, \overline{M})} \\
&= \mathbb{P}^{\mathfrak{C}}(M|x, T) \left(\mathbb{P}^{\mathfrak{C}}(Y|x, M) - \mathbb{P}^{\mathfrak{C}}(Y|x, \overline{M}) \right).
\end{aligned}$$

which completes the proof. ■

A.4 Proposition 3

Single-stratum setting. We focus on the IPE estimation for a single value x_0 of X , for which we assume to observe n *i.i.d.* samples $\{(x_0, T_i, M_i, Y_i)\}_{1 \leq i \leq n}$.

Notations. Consistently with notations presented in Equations 4, $\alpha(x_0)$, $\beta(x_0)$ refer respectively to the relative IPE and relative ITE in stratum $\{X = x_0\}$ (and are assumed to be positive in this illustrative setting), and we denote $\hat{\gamma}(x_0)$, $\hat{\tau}^{IPE}(x_0)$ and $\hat{\tau}^{ITE}(x_0)$ respectively the maximum-likelihood estimator (MLE) of $\gamma(x_0)$, and the MLE-based two-model estimators (difference of two MLE estimators) of $\tau^{IPE}(x_0)$ and $\tau^{ITE}(x_0)$. We define the associated C-IPE estimator as $\hat{\tau}^{C-IPE}(x_0) \triangleq \hat{\gamma}(x_0)\hat{\tau}^{ITE}(x_0)$. Lastly, we denote $p_1(x_0) = \mathbb{P}^{\mathfrak{C}}(Y|T, x_0)$.

In Proposition 3, we present an asymptotic bound for the ratio of the standard deviation (sd) of C-IPE and IPE estimators (additionally assuming $\mathbb{P}^{\mathfrak{C}}(T) = \frac{1}{2}$ for simplicity), namely:

$$\lim_{n \rightarrow \infty} \frac{\text{sd}(\hat{\tau}^{C-IPE}(x_0))}{\text{sd}(\hat{\tau}^{IPE}(x_0))} \leq \sqrt{\left(\frac{2(1 + \beta(x_0))}{(1 - p_1(x_0))(2 + \alpha(x_0))} \right) \gamma(x_0)}$$

Proof.

The proof is splitted in four steps:

1. Maximum-Likelihood and treatment effect estimators
2. Variance of estimators derivation
3. Variance upper and lower bounds
4. Wrap up

Every random quantity is henceforth implicitly considered to be ‘with respect to x_0 ’.

1. Maximum-Likelihood and treatment effect estimators We remind that for two categorical random variables X and Y , for which we observe n *i.i.d.* samples $\{(X_i, Y_i)\}_{1 \leq i \leq n}$, we have the following Maximum-Likelihood estimators for $p(x) = P(X = x)$, $p(x, y) = P(X = x, Y = y)$ and $p(y|x) = P(X = x|Y = y)$:

$$\begin{aligned} \hat{p}(x) &= \frac{1}{n} \sum_{i=1}^n \mathbb{I}_{X_i=x} \\ \hat{p}(x, y) &= \frac{1}{n} \sum_{i=1}^n \mathbb{I}_{X_i=x} \mathbb{I}_{Y_i=y} \\ \hat{p}(y|x) &= \frac{\sum_{i=1}^n \mathbb{I}_{X_i=x} \mathbb{I}_{Y_i=y}}{\sum_{i=1}^n \mathbb{I}_{X_i=x}}. \end{aligned} \tag{11}$$

Since $\sum_{i=1}^n \mathbb{I}_{X_i=x} = 0 \Rightarrow \sum_{i=1}^n \mathbb{I}_{X_i=x} \mathbb{I}_{Y_i=y} = 0$, we adopt the convention $\hat{P}(X = x|Y = y) = 0$ in case of null denominator for a ratio estimator such as $\hat{p}(X = x|Y = y)$, ensuring they are well defined for any samples.

In our context, we have n *i.i.d.* samples $\{(T_i, M_i, Y_i)\}_{1 \leq i \leq n}$ of variables (T, M, Y) , and that we suppose $\mathbb{P}^{\mathfrak{C}}(T) = \frac{1}{2}$.

We first define the following compact notations:

$$\begin{aligned} t &= \mathbb{P}^{\mathfrak{C}}(T) & \gamma &= \mathbb{P}^{\mathfrak{C}}(M|T) \\ p_0 &= \mathbb{P}^{\mathfrak{C}}(Y|\overline{T}) & p_1 &= \mathbb{P}^{\mathfrak{C}}(Y|T) \\ q_0 &= \mathbb{P}^{\mathfrak{C}}(Y|\overline{M}) & q_1 &= \mathbb{P}^{\mathfrak{C}}(Y|M) \end{aligned}$$

Associated MLEs $\hat{p}_0, \hat{p}_1, \hat{q}_0, \hat{q}_1, \hat{t}$ and $\hat{\gamma}$ are given by Equations (11). For instance:

$$\begin{aligned} \hat{t} &= \frac{1}{n} \sum_{i=1}^n T_i & \hat{\gamma} &= \frac{1}{\sum_{i=1}^n T_i} \sum_{i=1}^n M_i \\ \hat{p}_0 &= \frac{1}{\sum_{i=1}^n (1 - T_i)} \sum_{i=1}^n (1 - T_i) Y_i & \hat{p}_1 &= \frac{1}{\sum_{i=1}^n T_i} \sum_{i=1}^n T_i Y_i \\ \hat{q}_0 &= \frac{1}{\sum_{i=1}^n (1 - M_i)} \sum_{i=1}^n (1 - M_i) Y_i & \hat{q}_1 &= \frac{1}{\sum_{i=1}^n M_i} \sum_{i=1}^n M_i Y_i \end{aligned}$$

Direct estimators for τ^{IPE}, τ^{ITE} are given by applying the two-model approach to MLEs given in these equations, *i.e.*

$$\begin{aligned} \hat{\tau}^{IPE} &= \hat{p}_1 - \hat{p}_0 \\ \hat{\tau}^{ITE} &= \hat{q}_1 - \hat{q}_0 \end{aligned}$$

and the corresponding τ^{C-IPE} estimator therefore writes:

$$\hat{\tau}^{C-IPE} = (\hat{q}_1 - \hat{q}_0) \hat{\gamma}.$$

In what follows, we will now write \sum_i instead of $\sum_{i=1}^n$ when there is no ambiguity.

2. Variance of estimators derivation

2.a. $\hat{\tau}^{IPE}$ variance derivation

For any random variables X, Y , we remind that:

$$\text{Var}(X) = \text{Var}(\mathbb{E}[X|Y]) + \mathbb{E}[\text{Var}(X|Y)]. \quad (12)$$

Which applied with $X = \hat{\tau}^{IPE} = \hat{p}_1 - \hat{p}_0$ and $Y = \{T_k\}_k := \{T_1, \dots, T_n\}$, gives:

$$\text{Var}(\hat{\tau}^{IPE}) = \underbrace{\mathbb{E} [\text{Var}(\hat{\tau}^{IPE} | \{T_k\}_k)]}_{\textcircled{\text{A}}} + \underbrace{\text{Var} [\mathbb{E}(\hat{\tau}^{IPE} | \{T_k\}_k)]}_{\textcircled{\text{B}}}. \quad (13)$$

Computation of $\textcircled{\text{A}}$

The term $\text{Var}(\hat{\tau}^{IPE} | \{T_k\}_k)$ decomposes as:

$$\text{Var}(\hat{\tau}^{IPE} | \{T_k\}_k) = \underbrace{\text{Var}(\hat{p}_1 | \{T_k\}_k)}_{\textcircled{\text{A1}}} + \underbrace{\text{Var}(\hat{p}_0 | \{T_k\}_k)}_{\textcircled{\text{A2}}} - 2 \underbrace{\text{Cov}(\hat{p}_1, \hat{p}_0 | \{T_k\}_k)}_{\textcircled{\text{A3}}}. \quad (14)$$

For (A1), we write:

$$\begin{aligned}
\text{Var}(\hat{p}_1|\{T_k\}_k) &= \text{Var}\left(\frac{1}{\sum_i T_i} \sum_i T_i Y_i | \{T_k\}_k\right) \\
&= \left(\frac{1}{\sum_i T_i}\right)^2 \text{Var}\left(\sum_i T_i Y_i | \{T_k\}_k\right) \\
&= \left(\frac{1}{\sum_i T_i}\right)^2 \sum_i \text{Var}(T_i Y_i | \underbrace{\{T_k\}_k}_{T_i \text{ (since i.i.d.)}}) \\
&= \left(\frac{1}{\sum_i T_i}\right)^2 \sum_i \underbrace{T_i \text{Var}(Y_i | T_i)}_{\text{Var}(Y|T=1) T_i \text{ (since i.i.d.)}} \\
&= \left(\frac{1}{\sum_i T_i}\right)^2 \text{Var}(Y|T=1) \sum_i T_i \\
&= \frac{1}{\sum_i T_i} \text{Var}(Y|T=1) \\
&= \frac{1}{\sum_i T_i} p_1(1-p_1).
\end{aligned}$$

For (A2), we analogously get:

$$\text{Var}(\hat{p}_0|\{T_k\}_k) = \frac{1}{\sum_i (1-T_i)} p_0(1-p_0).$$

For (A3), using the bi-linearity of covariance, we write:

$$\begin{aligned}
\text{Cov}(\hat{p}_1, \hat{p}_0|\{T_k\}_k) &= \text{Cov}\left(\frac{1}{\sum_i T_i} \sum_i T_i Y_i, \frac{1}{\sum_j (1-T_j)} \sum_j (1-T_j) Y_j | \{T_k\}_k\right) \\
&= \frac{1}{\sum_i T_i} \frac{1}{\sum_j (1-T_j)} \text{Cov}\left(\sum_i T_i Y_i, \sum_j (1-T_j) Y_j | \{T_k\}_k\right) \\
&= \frac{1}{\sum_i T_i} \frac{1}{\sum_j (1-T_j)} \sum_i \sum_j (1-T_j) T_i \underbrace{\text{Cov}(Y_i, Y_j | \{T_k\}_k)}_{\neq 0 \text{ only if } i=j \text{ (since i.i.d.)}} \\
&= \frac{1}{\sum_i T_i} \frac{1}{\sum_j (1-T_j)} \sum_i (1-T_i) T_i \text{Cov}(Y_i, Y_i | \underbrace{\{T_k\}_k}_{T_i \text{ (since i.i.d.)}}) \\
&= \frac{1}{\sum_i T_i} \frac{1}{\sum_j (1-T_j)} \sum_i \underbrace{(1-T_i) T_i}_{=0} \text{Var}(Y_i | T_i) \\
&= 0.
\end{aligned}$$

Injecting values of (A1), (A2) and (A3) in Equation (14) we get:

$$\text{Var}(\hat{\tau}^{IPE}|\{T_k\}_k) = \frac{1}{\sum_i T_i} p_1(1-p_1) + \frac{1}{\sum_i (1-T_i)} p_0(1-p_0). \quad (15)$$

Which leads to the following expression for (A):

$$\mathbb{E} [\text{Var}(\hat{\tau}^{IPE}|\{T_k\}_k)] = \mathbb{E} \left[\frac{1}{\sum_i T_i} \right] p_1(1 - p_1) + \mathbb{E} \left[\frac{1}{\sum_i (1 - T_i)} \right] p_0(1 - p_0). \quad (16)$$

Computation of (B)

We may write

$$\mathbb{E}(\hat{\tau}^{IPE}|\{T_k\}_k) = \underbrace{\mathbb{E}(\hat{p}_1|\{T_k\}_k)}_{(B1)} - \underbrace{\mathbb{E}(\hat{p}_0|\{T_k\}_k)}_{(B2)}.$$

For (B1), we write:

$$\begin{aligned} \mathbb{E}(\hat{p}_1|\{T_k\}_k) &= \mathbb{E} \left(\frac{1}{\sum_i T_i} \sum_i T_i Y_i | \{T_k\}_k \right) \\ &= \frac{1}{\sum_i T_i} \sum_i \mathbb{E}(T_i Y_i | \{T_k\}_k) \\ &= \frac{1}{\sum_i T_i} \sum_i T_i \underbrace{\mathbb{E}(Y_i | T_i)}_{p_1} \\ &= \frac{1}{\sum_i T_i} \left(\sum_i T_i \right) p_1 \\ &= p_1. \end{aligned}$$

For (B2), we analogously get: $\mathbb{E}(\hat{p}_0|\{T_k\}_k) = p_0$.

Therefore $\mathbb{E}(\hat{\tau}^{IPE}|\{T_k\}_k) = p_1 - p_0$ is constant relatively to $\{T_k\}_k$, and we have computed (B):

$$\text{Var} [\mathbb{E}(\hat{\tau}^{IPE}|\{T_k\}_k)] = 0. \quad (17)$$

Combining Equations (13), (16) and (17) we end up with:

$$\text{Var}(\hat{\tau}^{IPE}) = \mathbb{E} \left[\frac{1}{\sum_i T_i} \right] p_1(1 - p_1) + \mathbb{E} \left[\frac{1}{\sum_i (1 - T_i)} \right] p_0(1 - p_0). \quad (18)$$

2.b. $\hat{\tau}^{C-IPE}$ variance derivation

Using Equation (12) with $X = \hat{\tau}^{C-IPE} = \hat{\gamma}(\hat{q}_1 - \hat{q}_0)$ and $Y = \{T_k, M_k\}_k$ we may write:

$$\text{Var}(\hat{\tau}^{C-IPE}) = \underbrace{\mathbb{E} [\text{Var}(\hat{\tau}^{C-IPE}|\{T_k, M_k\}_k)]}_{(C)} + \underbrace{\text{Var} [\mathbb{E}(\hat{\tau}^{C-IPE}|\{T_k, M_k\}_k)]}_{(D)}. \quad (19)$$

Computation of (C)

Using the fact that $\hat{\tau}^{C-IPE} = \hat{\gamma}(\hat{q}_1 - \hat{q}_0)$, and remarking that $\mathbb{E}[\hat{\gamma}|\{T_k, M_k\}_k] = \hat{\gamma}$, we may write:

$$\text{Var}(\hat{\gamma}(\hat{q}_1 - \hat{q}_0)|\{T_k, M_k\}_k) = \hat{\gamma}^2 \text{Var}((\hat{q}_1 - \hat{q}_0)|\{T_k, M_k\}_k)$$

By analogy with Equation (15), we have

$$\text{Var}(\hat{q}_1 - \hat{q}_0 | \{T_k, M_k\}_k) = \frac{1}{\sum_i M_i} q_1(1 - q_1) + \frac{1}{\sum_i (1 - M_i)} q_0(1 - q_0),$$

which gives

$$\text{Var}(\hat{\gamma}(\hat{q}_1 - \hat{q}_0) | \{T_k, M_k\}_k) = \hat{\gamma}^2 \left(\frac{1}{\sum_i M_i} q_1(1 - q_1) + \frac{1}{\sum_i (1 - M_i)} q_0(1 - q_0) \right). \quad (20)$$

Injecting $\hat{\gamma} = \frac{\sum_i M_i}{\sum_i T_i} = \frac{\sum_i M_i T_i}{\sum_i T_i}$ in (20), we get:

$$\text{Var}(\hat{\gamma}(\hat{q}_1 - \hat{q}_0) | \{T_k, M_k\}_k) = \frac{\sum_i M_i}{(\sum_i T_i)^2} q_1(1 - q_1) + \frac{(\sum_i M_i)^2}{(\sum_i T_i)^2 \sum_i (1 - M_i)} q_0(1 - q_0).$$

Taking the expectancy, we therefore get the following expression for $\textcircled{\text{C}}$:

$$\mathbb{E} [\text{Var}(\hat{\tau}^{C-IP E} | \{T_k, M_k\}_k)] = \mathbb{E} \left[\frac{\sum_i M_i}{(\sum_i T_i)^2} \right] q_1(1 - q_1) + \mathbb{E} \left[\frac{(\sum_i M_i)^2}{(\sum_i T_i)^2 \sum_i (1 - M_i)} \right] q_0(1 - q_0). \quad (21)$$

Computation of $\textcircled{\text{D}}$

Using the fact that $\hat{\gamma}$ is $\{T_k, M_k\}_k$ -measurable, we get:

$$\mathbb{E}(\hat{\tau}^{C-IP E} | \{T_k, M_k\}_k) = \hat{\gamma} \underbrace{(\mathbb{E}(\hat{q}_1 | \{T_k, M_k\}_k))}_{\textcircled{\text{D1}}} - \underbrace{\mathbb{E}(\hat{q}_0 | \{T_k, M_k\}_k)}_{\textcircled{\text{D2}}}. \quad (22)$$

For $\textcircled{\text{D1}}$, a few mechanical computations bring:

$$\begin{aligned} \mathbb{E}(\hat{q}_1 | \{T_k, M_k\}_k) &= \mathbb{E} \left(\frac{1}{\sum_i M_i} \sum_i M_i Y_i | \{T_k, M_k\}_k \right) \\ &= \frac{1}{\sum_i M_i} \mathbb{E} \left(\sum_i M_i Y_i | \{T_k, M_k\}_k \right) \\ &= \frac{1}{\sum_i M_i} \sum_i M_i \mathbb{E}(Y_i | \{T_k, M_k\}_k) \\ &= \frac{1}{\sum_i M_i} \sum_i \underbrace{M_i \mathbb{E}(Y_i | T_i, M_i)}_{M_i \mathbb{E}[Y | M=1]} \\ &= \underbrace{\mathbb{E}[Y | M=1]}_{q_1} \frac{1}{\sum_i M_i} \sum_i M_i \\ &= q_1 \end{aligned}$$

For $\textcircled{\text{D2}}$, we analogously get:

$$\mathbb{E}(\hat{q}_0 | \{T_k, M_k\}_k) = q_0.$$

Injecting these values in (22):

$$\mathbb{E}(\hat{\tau}^{C-IP E} | \{T_k, M_k\}_k) = \hat{\gamma}(q_1 - q_0).$$

which gives the following expression for $\textcircled{\text{D}}$:

$$\text{Var}(\mathbb{E}(\hat{\tau}^{C-IP E}|\{T_k, M_k\}_k)) = (q_1 - q_0)^2 \text{Var}(\hat{\gamma}).$$

Using the fact that $\text{Var}(\hat{\gamma}) = \mathbb{E}(\text{Var}(\hat{\gamma}|\{T_k\})) + \text{Var}(\mathbb{E}[\hat{\gamma}|\{T_k\}])$, we get:

$$\text{Var}(\hat{\gamma}) = \mathbb{E}\left(\frac{1}{\sum_i T_i}\right) \gamma(1 - \gamma).$$

We end up with the final expression for $\textcircled{\text{D}}$:

$$\text{Var}(\mathbb{E}[\hat{\tau}^{C-IP E}|\{T_k, M_k\}_k]) = (q_1 - q_0)^2 \mathbb{E}\left[\frac{1}{\sum_i T_i}\right] \gamma(1 - \gamma). \quad (23)$$

Combining Equations (19), (21) and (23), we have:

$$\text{Var}(\hat{\tau}^{C-IP E}) = \mathbb{E}\left[\frac{\sum_i M_i}{(\sum_i T_i)^2}\right] q_1(1 - q_1) + \mathbb{E}\left[\frac{(\sum_i M_i)^2}{(\sum_i T_i)^2 \sum_i (1 - M_i)}\right] q_0(1 - q_0) + (q_1 - q_0)^2 \mathbb{E}\left(\frac{1}{\sum_i T_i}\right) \gamma(1 - \gamma). \quad (24)$$

3. Asymptotic variance upper and lower bounds

3.a Asymptotic lower bound of $\text{Var}(\hat{\tau}^{IP E})$ With a slight rewriting of (18),

$$n \text{Var}(\hat{\tau}^{IP E}) = \mathbb{E}\left[\frac{1}{\frac{1}{n} \sum_i T_i}\right] p_1(1 - p_1) + \mathbb{E}\left[\frac{1}{\frac{1}{n} \sum_i (1 - T_i)}\right] p_0(1 - p_0).$$

Then because $t = \mathbb{P}^{\mathcal{C}}(T) = \frac{1}{2}$, by the law of large numbers, we get

$$\lim_{n \rightarrow \infty} n \text{Var}(\hat{\tau}^{IP E}) = 2(p_1(1 - p_1) + p_0(1 - p_0)). \quad (25)$$

Now, using $p_1 = (1 + \alpha)p_0$, we can write:

$$\begin{aligned} \lim_{n \rightarrow \infty} n \text{Var}(\hat{\tau}^{IP E}) &= 2p_0(1 - p_0 + (1 + \alpha)(1 - p_1)) \\ &\geq 2p_0(1 - p_1 + (1 + \alpha)(1 - p_1)) \\ &= 2p_0(1 - p_1)(2 + \alpha), \end{aligned}$$

where the first inequality uses $\alpha \geq 0$. In summary, we have the following asymptotic lower bound for $\text{Var}(\hat{\tau}^{IP E})$:

$$\lim_{n \rightarrow \infty} n \text{Var}(\hat{\tau}^{IP E}) \geq 2p_0(1 - p_1)(2 + \alpha). \quad (26)$$

3.a Asymptotic upper bound of $\text{Var}(\hat{\tau}^{C-IP E})$

From (24), we have

$$\begin{aligned} n \text{Var}(\hat{\tau}^{C-IP E}) &= \mathbb{E}\left[\frac{\frac{1}{n} \sum_i M_i}{(\frac{1}{n} \sum_i T_i)^2}\right] q_1(1 - q_1) + \mathbb{E}\left[\frac{(\frac{1}{n} \sum_i M_i)^2}{(\frac{1}{n} \sum_i T_i)^2 \frac{1}{n} \sum_i (1 - M_i)}\right] q_0(1 - q_0) \\ &\quad + (q_1 - q_0)^2 \mathbb{E}\left(\frac{1}{\frac{1}{n} \sum_i T_i}\right) \gamma(1 - \gamma). \end{aligned} \quad (27)$$

Again, using the law of large numbers, we get

$$\lim_{n \rightarrow \infty} n \text{Var}(\hat{\tau}^{C-IP E}) = 2\gamma q_1(1 - q_1) + 2\frac{\gamma^2}{2 - \gamma} q_0(1 - q_0) + 2\gamma(1 - \gamma)(q_1 - q_0)^2. \quad (28)$$

Now, using that for any $q \in [0, 1]$, $q(1 - q) \leq q$, and reminding that $q_1 = (1 + \beta)q_0 \leq 1$ where $\beta \geq 0$ by assumption, we get:

$$\begin{aligned}
\lim_{n \rightarrow \infty} n \text{Var}(\hat{\tau}^{C-IP E}) &= 2\gamma q_1(1 - q_1) + 2\frac{\gamma^2}{2 - \gamma} q_0(1 - q_0) + 2\gamma(1 - \gamma)(q_1 - q_0) \\
&\leq 2\gamma \left(\underbrace{q_1}_{\leq q_0} + \underbrace{\frac{\gamma}{2 - \gamma} q_0}_{\leq \gamma \leq 1} + \underbrace{(q_0(1 + \beta))^2}_{\leq q_0(1 + \beta)} \right) \\
&\leq 2\gamma q_0(1 + \beta + 1 + \beta) \\
&= 4q_0\gamma(1 + \beta).
\end{aligned}$$

In summary, we have the following asymptotic upper bound for $\text{Var}(\hat{\tau}^{C-IP E})$:

$$\lim_{n \rightarrow \infty} n \text{Var}(\hat{\tau}^{C-IP E}) \leq 4q_0\gamma(1 + \beta). \quad (29)$$

4. Wrap up

Combining Equations (26) and (29) (ratio of positive values), we get

$$\begin{aligned}
\frac{\lim_{n \rightarrow \infty} n \text{Var}(\hat{\tau}^{C-IP E})}{\lim_{n \rightarrow \infty} n \text{Var}(\hat{\tau}^{IP E})} &\leq \frac{4q_0\gamma(1 + \beta)}{2p_0(1 - p_1)(2 + \alpha)} \\
&= 2 \frac{1 + \beta}{(1 - p_1)(2 + \alpha)} \gamma.
\end{aligned}$$

Where we remind that *One-sided non-compliance* and *Exclusive treatment effect* imply straightforwardly that $p_0 = q_0$ (as shown in the beginning of the proof of Proposition 2). Since the limits of both the numerator and denominator exist, this implies that

$$\lim_{n \rightarrow \infty} \frac{\text{Var}(\hat{\tau}^{C-IP E})}{\text{Var}(\hat{\tau}^{IP E})} \leq 2 \frac{1 + \beta}{(1 - p_1)(2 + \alpha)} \gamma.$$

Taking the square root of this equation gives the wanted result. ■

B Additional Results and Experimentation Details

B.1 AUUC

AUUC (Rzepakowski & Jaroszewicz, 2012, 2010; Radcliffe & Surry, 2011) is the Area Under the Uplift Curve. It is obtained by ranking the users of a test set according to their predicted uplift, in descending order.

The uplift curve starts at the point $(0, 0)$, then for each user (in decreasing order of the predicted uplift) it goes up of 1 point if the user is in group $T = 1$ with $Y = 1$, it goes down of 1 point if the user is in group $T = 0$ with $Y = 1$, and it stays flat if the user has $Y = 0$. So the label l is $Y * (2T - 1)$. We normalise the x-axis so that it goes from 0 to 1.

The aim of uplift model is to rank first the users with positive outcome in treatment ($T = 1$), then the users with negative outcome, and finally the users with positive outcome not in treatment ($T = 0$). Thus, the area under the uplift curve is maximal.

However the value of the AUUC highly depends on the test set. Indeed the first point of the uplift curve is always $(0, 0)$ and the last one is always $(1, U)$ where $U = \sum YT - \sum Y(1 - T)$. Therefore the variability of the test set (when we do different splits) accounts for part of the variability of the metrics. To reduce this variability, we subtract the average AUUC of a random model (which is equal to $\frac{U}{2}$) from the AUUC of tested models. This measure is called ΔAUUC .

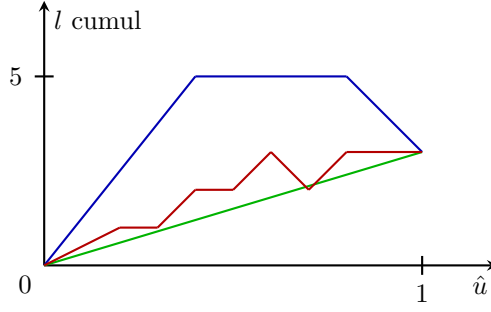


Figure 7: Example of uplift curves. The blue line corresponds to a perfect model, the green line is the expectation of a random model and the red line is an example of a model. The AUUC is the area under those curves.

B.2 Models training

Our goal is to compare the IPE (Individual Treatment Effect) approach with C-IPE (post-Mediation Individual Treatment Effect) approach. We implement two kinds of model for both IPE and ITE (Individual Treatment Effect if Treated) factor of C-IPE. These models are (1) the Two-Models, with one model learnt on the group $T = 1$ and one model learnt on the group $T = 0$, and (2) Shared Data Representation (SDR), from Betlei et al. (2018), which is inspired from multi-task learning and has more capacity than the basic Two-Models approach.

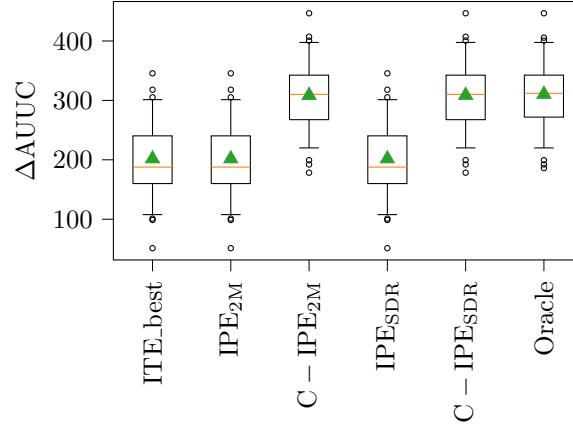


Figure 8: Δ AUUC (higher is better) of two IPE models, corresponding C-IPE models and Oracle model (theoretical truth). Box plots are done on 51 random splits, whiskers at 5/95 percentiles. Note how C-IPE systematically increases AUUC of base estimators

On synthetic data, we also compare the models to two theoretical models: IPE_{best} and Oracle:

- IPE_{best} is the best possible model learn-able using training data but without exploiting information from the mediation variable M . In short, this model predicts the difference of the empirical positive outcome rate in the group $T = 1$ and in the group $T = 0$ and does so in each category of users. This is a rightful approach in the case of our synthetic dataset, since we observe a high number of users for each possible category (each value of x). It is the best possible model learnt, because the dataset is generated with one different probability of positive outcome per category: there is nothing else any model could learn without exploiting variable M .

IPE_{best} allows us to show that, in our synthetic dataset, two models and SDR perform close to the best possible IPE approach. In that specific low-dimensional case, there is therefore no need to implement more complex models (Figure 8) such as doubly-robust methods or tree/forest-based methods.

- Oracle predicts the theoretical ground truth uplift (used to generate the dataset). Its score is important since it represents the maximum theoretically reachable score (on average). In practice, we observe that it is however not the best model on all random splits. This can be explained by the fact that the (test) dataset is randomly generated, and that the ranking of users in the test set can therefore differ slightly from the theoretical ranking.

All learnt models (IPE, C-IPE and IPE_{best}) suffer from the randomness of the training dataset.

B.3 Models testing

In addition of the randomness of the training dataset, the test dataset is also random. This adds noise to the AUUC values that are computed in practice. We design a metric called, $\text{AUUC}_{\text{thout}}$ that computes the AUUC on a theoretical test set. This metric may only be implemented on synthetic data. It uses the "Theoretical Outcome" (thout) of each category of users as a label, thus circumventing the randomness inherent to the test set generation.

Figure 9 represents the performance of the same models as in Figure 8 but with the $\text{AUUC}_{\text{thout}}$ metric (AUUC on a theoretical test set). As expected the Oracle has no variance because it does not

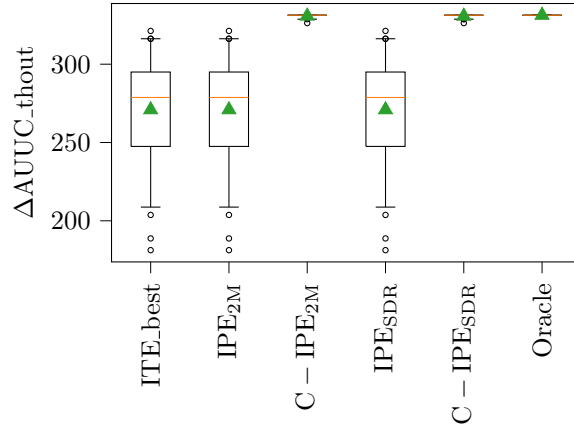


Figure 9: $\Delta \text{AUUC}_{\text{thout}}$ (higher is better) of two IPE models, corresponding C-IPE models and Oracle model (theoretical truth). Box plots are done on 51 random splits, whiskers at 5/95 percentiles. Note how C-IPE systematically increases AUUC of base estimators

suffer from the randomness of the training set (by design) and the $\text{AUUC}_{\text{thout}}$ metric gets rid of the variance of the test set. C-IPE models also have little to no $\text{AUUC}_{\text{thout}}$ variance in practice. This can be explained by the fact that these models learn the post mediation (ITE) signal, which is far less noisy than the IPE signal in low-compliance cases, and therefore suffer from less random variation.

B.4 Hyper-parameters tuning

For the open dataset CRITEO-UPLIFT¹², we first fit the compliance model $\hat{\gamma}(x)$ estimating the true individual compliance $\gamma(x) = \mathbb{P}^{\mathcal{C}; \text{do}(T)}(M|x)$ probability, from a separate process. Specifically, $\hat{\gamma}(x)$

¹²<http://cail.criteo.com/criteo-uplift-prediction-dataset/>

model is fitted directly as we have access to the compliance label M . We use a rebalanced LLH, as the classes $M = 1$ and $M = 0$ are very imbalanced. This step is crucial, as a good $\hat{\gamma}$ model ensures the superiority of C-IPE-based algorithms. The models are implemented using the logistic regression class, from Scikit-Learn Python library Pedregosa et al. (2011). We use for the hyper-parameter grid the Cartesian product of:

Table 4: Table of hyper-parameters for the compliance model

PARAMETER	VALUES
PENALTY REGULARIZATION	$\{L1, L2\}$
C : INVERSE OF REGULARIZATION STRENGTH	$\{0.01, 1, 10^2, 10^5\}$
CLASS_WEIGHT: WEIGHTS ASSOCIATED WITH CLASSES	$\{\text{BALANCED}, \text{NONE}\}$

Hyper-parameters are selected by internal 11-fold cross-validation on the training set by ranking by rebalanced log-likelihood as the model is predicting a probability. The best hyper-parameter triple found is L1 regularization, $C = 100$ and class_weight = 'balanced'.

In a second step, we tune the two individual treatment effect models $\hat{\gamma}^{IPE}$ and $\hat{\gamma}^{ITE}$, by doing again an internal cross-validation on the training set. We rank the hyper-parameters configuration by the delta AUUC metric, computed averaging over the different splits. The hyper-parameters grid is the Cartesian product of:

Table 5: Table of hyper-parameters for the individual treatment effect models

PARAMETER	VALUES
PENALTY REGULARIZATION	$\{L1, L2\}$
C : INVERSE OF REGULARIZATION STRENGTH	$\{0.01, 0.1, 1, 10, 10^2, 10^3, 10^4, 10^5\}$

Remark: for the plot of Figure 5, we only show the penalization L2, with an inverse regularization strength $C = 10$ as the ΔAUUC is found not sensitive to hyper-parameter (see subscript COMP in Table 6). Indeed the best hyper-parameters tuple (see subscript BEST in Table 6) for each method are the following:

Table 6: Table of hyper-parameters for the models. The metric is ΔAUUC

METHOD	C_{BEST}	$\text{PENALTY}_{\text{BEST}}$	$\Delta\text{AUUC}_{\text{BEST}}$	C_{COMP}	$\text{PENALTY}_{\text{COMP}}$	$\Delta\text{AUUC}_{\text{COMP}}$
IPE _{2M}	100000.0	L1	20484.044762	10.0	L2	20249.085940
IPE _{SDR}	1.0	L1	20596.476241	10.0	L2	20179.615970
C – IPE _{2M}	10.0	L2	21507.813960	10.0	L2	21507.813960
C – IPE _{SDR}	1.0	L2	21454.981632	10.0	L2	21333.441887

The corresponding performance the the best configuration are presented in Figure 10. Note that the order of magnitude for each method is very similar with the Figure 5, i.e. for penalization L2 and $C = 10$, which makes the fine tuning of the hyper-parameters unnecessary.

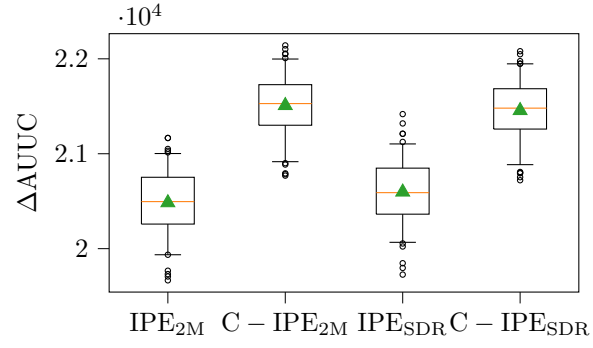


Figure 10: $\Delta AUUC$ (higher is better) for the best hyper-parameter configurations. Box plots are done on 100 random splits, whiskers at 5/95 percentiles. Note how C-IPE systematically increases $\Delta AUUC$ of IPE estimators

C Code

The full code used for (1) the experiments on synthetic data and (2) experiments on real-world open data described in this paper can be found in the `experiment_src.zip` file. The unzipped folder contains a `README.md` file that gives precise instructions enabling to re-run all experiments, and compare the results with the corresponding ones in the paper.